Раздел первый

ФИЗИКА РАДИАЦИОННЫХ ПОВРЕЖДЕНИЙ И ЯВЛЕНИЙ В ТВЕРДЫХ ТЕЛАХ

UDC 538.945

ANGULAR AND MAGNETIC FIELD DEPENDENCES OF CRITICAL CURRENT IN IRRADIATED YBaCuO SINGLE CRYSTALS

Yuri Petrusenko
National Science Center «Kharkov Institute of Physics & Technology», Kharkov, Ukraine

The investigation of mechanisms responsible for the current-carrying capability of irradiated high-temperature superconductors (HTSC) was realized. For the purpose, experiments were made to investigate the effect of point defects generated by high-energy electron irradiation on the critical temperature and the critical current in high-Tc superconducting single crystals $YBa_2Cu_3O_{7-x}$. The transport current density measured in HTSC single crystals $YBa_2Cu_3O_{7-x}$ by the dc-method was found to exceed 80000 A/cm^2. The experiments have demonstrated a more than 30-fold increase in the critical current density in single crystals irradiated with 2.5 MeV electrons to a dose of $3\cdot10^{18}$ el/cm^2. Detailed studies were made into the anisotropy of critical current and the dependence of critical current on the external magnetic field strength in irradiated single crystals. A high efficiency of point defects as centers of magnetic vortex pinning in HTSC single crystals was first demonstrated.

1. INTRODUCTION

As it follows from new expert conclusions, the use of superconducting materials in the 21st century will take on economic expediency and wide scale [1]. Undoubtedly, among different types of superconducting compounds, the use of which is gaining an intense progress, the high-temperature superconductors (HTSC) with a superconductor critical temperature of 90 to 100 K occupy a peculiar place owing to a possibility of using them at liquid nitrogen temperatures. Traditional low-temperature intermetallic superconductors require cooling down to liquid helium temperatures, and this significantly increases the expenses with their use.

Along with the superconductor critical temperature, a high critical current density is also one of the most important parameters that determine the degree of efficiency in the use of superconductors. As it is known, the transport critical current in HTSC single crystals and in single-domain quasi-monocrystalline samples is determined by special features of their structural defects. The main types of defects in single crystals are twin boundaries, dislocations, vacancies and impurity atoms. In polydomain crystal samples based on the 123-phase and in textured strips based on bismuth ceramics (2212-phase), the transport critical current is determined by weak intergranular bonds, i.e., by the state of boundaries (angle of grain disorientation, amount of oxygen, presence of impurities, etc.). In most cases, for the practical use of high-T_c superconductors it is their transport critical current that is of importance. However, it is also of importance to pay attention to the cases, where the quality of superconducting materials is determined by the intragranular critical current value, e.g., in the use of superconducting materials for the rotors of hysteretic HTSC motors [2]. In view of this, the results of studies on single crystals become of practical importance.

Many previous investigations, e.g., refs. [3-9], have demonstrated an efficiency of irradiation with fast neutrons and high-energy ions as a means of increasing the critical current in HTSC single crystals.

The aim of the present work has been to investigate the anisotropy and magnetic-field dependences of critical current in single crystals irradiated by high-energy electrons, i.e., to elucidate the special features of critical current versus the irradiation dose, the crystal orientation relative to the current vectors, versus the strength and value of the external magnetic field. These data are of crucial importance for the practical use of HTSC materials in real setups, devices or mechanisms, and can serve as a basis for the development of ecologically clean radiation technology to improve the current characteristics in high-T_c superconductors, including bulk polycrystalline materials.

By the present time it is well known that the irradiation by high-energy charged particles and neutrons to moderate doses, which are equivalent to a radiation defect concentration of 10^{-4} to 10^{-3} dpa, results in an increase of critical current in HTSC materials..

The effect of critical current rise has been attributed to the presence of additional magnetic-vortex pinning centers, the role of which belongs to radiation defects. It was considered in this case that it was the radiation damages with a large radius of action, such as defect clusters, tracks, etc., that were most efficient pinning centers, while point defects and their small clusters were not effective in the process. At the same time, it was neglected that one of the fundamental parameters of HTSC, namely, the coherence length, is small as compared to low-T_c superconductors and is $\xi \sim 10$ A. This may evidently determine the sensitivity of superconductivity parameters, such as critical current, when introducing small-radius defects, e.g., point defects, into the superconductor lattice. These defects can obviously be produced by irradiating

superconductors with ~0.5 to 10 MeV electrons. It should be also noted that the overwhelming majority of investigations on HTSC single crystals was performed for irradiation with neutrons and ions using the indirect method of critical current measurements, namely, magnetic susceptibility measurements. In this case, depending on the theoretical model chosen for critical current calculations, the J_c value could vary by factors of 10 to 100. Besides, the majority of irradiation experiments were performed at room temperature or at elevated temperatures, and this did not exclude the possibility of uncontrolled annealing of a part of radiation defects and complicated the interpretation of the resulting irradiation effects.

This paper is concerned with investigations into the influence of point defects on the critical current and the process of magnetic vortex pinning in high-quality $YBa_2Cu_3O_{7-x}$ single crystals, using a low-temperature (~ 10 K) irradiation by high-energy (2.5 MeV) electrons and the direct method of critical current measurements (from current-voltage characteristics).

2. EXPERIMENTAL TECHNIQUES

2.1. SAMPLES AND MEASURING TECHNIQUE

High-quality $YBa_2Cu_3O_{7-x}$ single crystals were prepared by the solution-melt method at temperature gradient conditions. The method of single crystal preparation has been described in detail in ref. [10]. The single crystals that had $T_c = 93$ K, $\Delta T_c = 0.3$ K and a resistivity of $\sim 6 \cdot 10^{-5}$ Ω·cm at T = 100 K were used to prepare samples for low-temperature electron irradiation and resistance measurements. The T_c value of single crystals was determined from temperature dependences of the resistivity in magnetic fields of intensity up to 5 T for different crystal orientations. The critical current density was determined from current-voltage characteristics (CVC). The measurements were performed before the irradiation and after each exposure to electrons. The samples for experiments were prepared in such a way that the current was always flowing in the crystallographic plane (ab) of the single crystal at an angle of 45° with respect to twin boundaries. The goniometric device provided the crystal orientation at any angle within the range from - 5 to 95° relative to the external magnetic field vector (for measurement procedures), and with the (ab) plane perpendicular to the electron beam (for irradiation). The transport critical current was found from the CVC for the electric field strengths $E = 10^{-5}$ V/cm (the current J_{c1}, which characterizes pinning inside creep regime) or $E = 4 \cdot 10^{-4}$ V/cm (the current J_{c2}, which characterizes pinning close to the depinning regime). The typical CVC for the initial and irradiated single crystal are presented in Fig. 1.

The measurements were carried out by the dc four-probe method using the precision digital voltmeters Schlumberger 7081 with a sensitivity of 10^{-8} V. A highly accurate electronic control system provided the regulation of sample temperature to an accuracy of 0.005 K. The software for the automated measuring system was performed in the VISUAL C^{++} programming environment. The experiment control program provides the measurements in both semiautomated- and automated regimes, control and registration of the parameters throughout the run permits the on-line representation of the data in the form of numerical tables and plots.

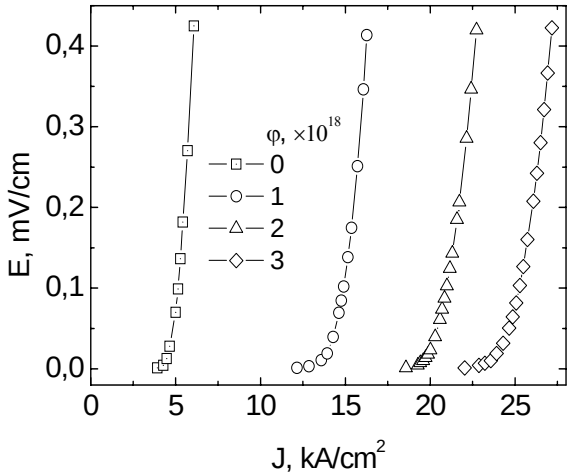

Fig. 1. Current-voltage characteristics of the single crystal irradiated with 2.5 MeV electrons at T = 10 K. The measurements were for T = 85 K, magnetic field H = 4 T, the (ab) crystal plane being parallel to the external magnetic field vector ($\alpha = \angle \mathbf{H}, ab = 0$)

2.2. RADIATION TECHNIQUE AT THE ELECTRON ACCELERATOR

HTSC single crystals were irradiated by 2.5 MeV electrons from the electrostatic electron accelerator, the density current being ~ 10 μA/cm². For irradiation at low temperatures and for precision measurements of electrophysical parameters of single crystals, a specially designed helium cryostat was used. It provided irradiation of crystals at a temperature not higher than 10 K, *in situ* measurements of temperature dependences of electrical resistivity and current-voltage characteristics in the temperature range from 10 to 400 K in magnetic fields with intensity up to 6 T. The electronic control system provided the temperature regulation in the measurements to an accuracy of 0.005 K. A special goniometric device provided the crystal alignment relative to both the electron beam (in irradiation) and the external magnetic field generated by the superconducting solenoid (in measurements).

3. RESULTS AND DISCUSSION

3.1. TEMPERATURE DEPENDENCES OF ELECTRICAL RESISTIVITY IN SINGLE CRYSTALS

The temperature dependences of electrical resistivity in the vicinity of superconductor critical temperatures are the vital characteristics responsible for the quality and physical state of the superconducting material. These dependences are of particular importance in deciding on the temperature range in the critical current measurements and in the interpretation of the results from these measurements.

Fig. 2 shows typical temperature dependences of the resistivity of $YBa_2Cu_3O_{7-x}$ single crystal before and after

irradiation with 2.5 MeV electrons at 10 K. The pre-irradiation measurements were performed in the absence of the magnetic field (H = 0). For the irradiated sample, the measurements were carried out for both H = 0 and for three typical orientations of the crystal plane (ab) relative to the magnetic field vector (α = 0, 14, 90°) for H = 15 kOe.

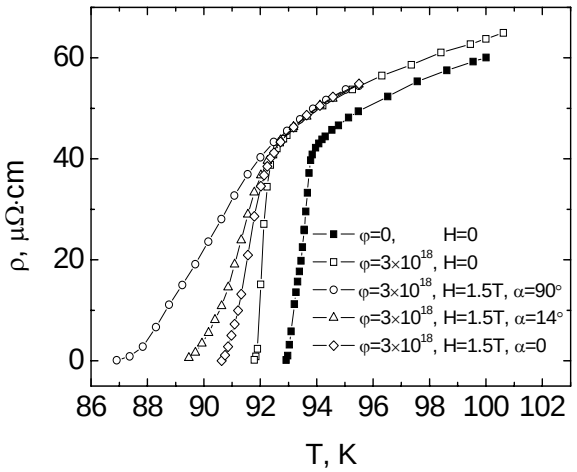

Fig. 2. Temperature dependences of resistivity of $YBa_2Cu_3O_{7-x}$ single crystal irradiated by 2.5 MeV electrons to a dose of $3\cdot10^{18}$ el/cm^2. The irradiation temperature is 10 K. The measurements are for H = 0 and H = 1.5 T for different crystal orientations

From the temperature curve of electrical resistivity of non-irradiated crystal the superconductor critical temperature and width were determined to be T_c = 93 K and ΔT_c = 0.3 K. The resistivity at 100 K was found to be about $6\cdot10^{-5}$ Ω·cm. These data characterize the sample as a high-quality one-phase superconducting single crystal, optimized in the composition.

For the irradiated crystal in the absence of the external magnetic field, the superconductor critical temperature is 1.3 K lower and the normal-state resistivity increases. In this case, the width of the superconducting transition does not change essentially, this being typical of HTSC at a moderate increase in the point defect concentration (up to ~ 10^{-4} dpa) [11, 12]. The external magnetic field dramatically changes the character of temperature curves, making them substantially broader, and the degree of broadening being much dependent on the field strength value and field orientation relative to the crystal. Thus for H = 1.5 T, the superconducting transition of the irradiated sample is extended to ~ 1.5 K. ~ 3 and ~ 5 K for the crystal orientations α = 0, 14 and 90°, respectively. The temperature, at which the resistivity of the sample fully disappears, i.e., the melting temperature of superconductor vortex lattice is lowered down to 90.6, 89.2 and 87 K, respectively. Our measurements at different magnetic field strengths up to 50 kOe confirm the above-mentioned peculiarities of temperature dependences of HTSC single-crystal resistivities. So, the decrease in the melting temperature of the vortex lattice is more dependent on the external magnetic field strength value and on the field orientation relative to crystallographic directions of the crystal than on the concentration of radiation-generated point defects. These results will be used in the interpretation of angular dependences (anisotropy) of critical current for electron-irradiated single crystals.

3.2. MAGNETIC-FIELD DEPENDENCES OF CRITICAL CURRENT AND THE DYNAMICS OF VORTEX LATTICE IN IRRADIATED SINGLE CRYSTALS

One of the most striking effects of electron irradiation is a sharp change in the behavior of critical current curves as functions of the external magnetic field (Fig. 3). The nonmonotonic function $J_c(H)$, i.e., the so-called "fish-tail" effect dramatically changes as early as after an irradiation dose of $1\cdot10^{18}$ el/cm^2. In this case, a sharply defined maximum appears at H = 30 kOe. With an increasing irradiation dose the maximum shifts towards lower magnetic fields and its amplitude grows.

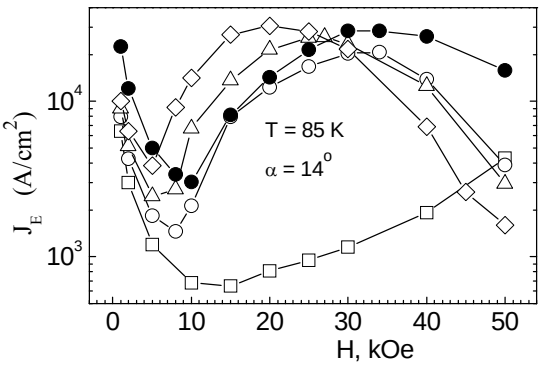

Fig. 3. Magnetic field dependence of critical current J_{c1} (light symbols) and J_{c2} (dark symbols) in the $YBa_2Cu_3O_{7-x}$ single crystal before (squares) and after irradiation with doses 10^{18} (circles), $2\cdot10^{18}$ (triangles) and $3\cdot10^{18}$ (diamonds). The measurements were performed for T = 85 K and α = 14°

It is believed that the position of the minimum on the $J_c(H)$ curves corresponds to the field H_{OD} that separates a low-field ordered and a high-field disordered state of the vortex lattice (VL). The nature of transition was discussed [13,14] in terms of the Lindemann criterion. By analogy with the transition from the liquid to the crystalline state, it was assumed that an order-disorder (OD) transition occurs in the crystalline VL if the transverse displacements u of the vortex lines exceed $c_L a_0$, where c_L is the Lindemann number, $a_0 \approx \sqrt{\Phi_0/B}$ is the intervortex distance, and Φ_0 is a quantum of magnetic flux. In terms of the cage potential model [13,14] which takes into account the interaction of the vortex line under consideration with a periodic potential created by the surrounding vortices, it was shown that the transverse displacement $u = c_L a_0$ increases the elastic energy of the VL by an amount

$$E_{el} = c_L^2 \varepsilon_0 a_0 . \qquad (1)$$

Here ε is the anisotropy parameter, $\varepsilon_0 = (\Phi_0/4\pi\lambda)^2$, and λ is the penetration depth of the magnetic field. Therefore an OD translation occurs if the energy E_{el} is compensated by the pinning energy E_p. When there is

pinning at the point defects, the pinning energy [13] $E_p \propto H^{-0.1}$ decreases with increasing field substantially more slowly than the energy $E_{el} \propto H^{-0.5}$. Consequently, in weak fields, the energy E_{el} exceeds the pinning energy, and the ordered state of the VL occurs, but in strong fields the pinning energy compensates the energy E_{el}, and the disordered state of the VL occurs. Therefore field H_{OD} is determined by the equal-energy condition $E_p = E_{el}$.

These theoretical predictions were confirmed by experimental studies of the high-temperature superconductors. Structural studies of the VLs in BiCaSrCuO crystals [15] and $YBa_2Cu_3O_{7-}$ crystals [16] showed that the low-field ordered state of the VL changes to the disordered state as H increases. A comparison of the field dependence of the pinning force in BiCaSrCuO crystals [17] and YBaCuO crystals [16] and of the structural changes of the VLs in these crystals, showed that the low-field ordered state of the VLs corresponds to a decrease of the force F_P as H increases, whereas, when the disordered state occurs in large fields, the force F_P increases with magnetic field.

It is assumed that the pinning force of the ordered VL decreases with increasing field because of the increase of the intervortex interaction, and this degrades the adaptation of the vortices to the landscape of the pinning centers. When the state becomes disordered, a definite role is apparently played by VL dislocations. First, the screw components of the dislocations initiate entanglement of the vortex lines and consequently produce dimensional crossover of the pinning force [13,18], i.e. a transition from 1D pinning of the ordered VL to 3D pinning of the disordered VL. Second, dislocations of the VL produce additional degrees of freedom for the transverse deformations of the vortex lines, and this improves the adaptation of the VL to the landscape of the pinning centers [19].

As can be seen in Fig. 3, as concentration n_{pd} increases, the H_{OD} field decreases, and this agrees with the results of the earlier experimental studies [9]. Such behavior conforms to expectations, taking into account that the pinning energy increases with the defect concentration [20] $E_p \propto n_{pd}^{1/3}$, while the energy $E_{el} = c_L^2 \varepsilon_0 a_0$ remains unchanged. The larger pinning energy can compensate the larger gain in elastic energy of the VL; therefore, the OD transition shifts into the region of smaller fields as the point-defect concentration increases.

The phase states of the static and dynamic VLs differ from each other. It was proposed in the pioneering work of Koshelev and Vinokur [21] that, as the velocity υ of the vortices increases above some critical value υ_c, a dynamic phase transition occurs from the disordered state of the VL to the state of a vortex crystal. It was later shown [22] that increasing the velocity υ suppresses the pinning effect only in the longitudinal direction (with respect to vector $\mathbf{\upsilon}$), while the pinning barriers remain finite in the transverse direction. This results in the formation of static longitudinal channels of motion of the vortices, which have been experimentally observed in $NbSe_2$ crystals [23] and in papers on the modelling of moving VLs [24]. Experimental studies of how the dynamic ordering of the VL affects the field dependence of the pinning force were carried out on crystals of $NbSe_2$ [25], V_3Si [26], and $YBa_2Cu_3O_{7-\delta}$ [27]. It was shown that the $F_p(H)$ dependences measured at low and high velocities υ differ from each other. In particular, in $YBa_2Cu_3O_{7-\delta}$ crystals measured for magnetic field parallel to the **c** axis [27] and in inclined magnetic fields [28], the minimum on the dependence shifts into the higher-field region with increasing velocity υ, and this is interpreted as the partial dynamic ordering of the VL. Therefore we believe that difference in the peak position on the $J_{c1}(H)$ and $J_{c2}(H)$ curves, which is observed in Fig.3, is caused by partial dynamic ordering.

At low magnetic fields ($H < H_{OD}$), the current dependence of the activation energy $U(J)$ is in good agreement with the theory of collective pinning [20], while at high magnetic fields ($H > H_{OD}$) the $U(J)$ dependence is consistent with the plastic creep theory, which is based on the concept of thermally-activated motion of vortex lattice dislocations [29]. This is demonstrated in Fig. 4, which shows $E(J)$ dependences plotted in the $\log E - \log J$ scale.

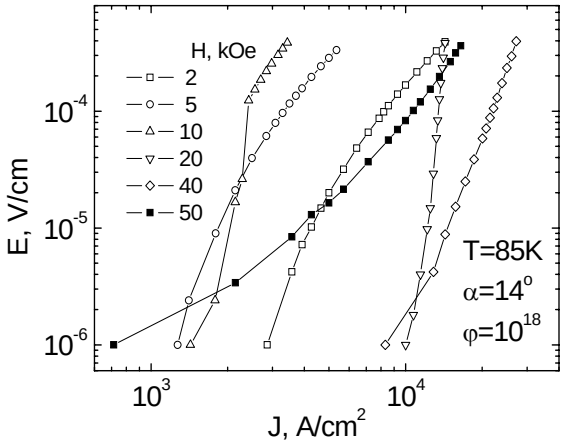

Fig. 4. Current-voltage characteristics measured after irradiation with a dose of 10^{18}

In low fields, $H < 10$ kOe, the $E(J)$ curve exhibits negative curvature, while in high fields, $H > 10$ kOe, the $E(J)$ curves exhibit positive curvature. This means that thermal creep is described by equation

$$E(J) \propto \exp\left[-(U_0/k_BT)(J_d/J)^{\mu}\right],$$

where the exponent μ is positive in low fields, as it is predicted by the theory of collective pinning for the elastic creep, but the exponent μ is negative in high fields, as it is predicted for the plastic creep mediated by motion of the vortex lattice dislocations [29]. Note, that in magnetic field 10 kOe the $E(J)$ dependence has the positive curvature at small currents, while at high current it has negative curvature. This peculiarity is strong evidence of the dynamic ordering: slow moving

disordered VL transforms into fast moving partially ordered VL.

The effects of irradiation on the pinning characteristics have been described in detail for measurements performed in magnetic field $\mathbf{H} \| \mathbf{c}$ [30]. These results have enabled to trace the transition from the mechanism of elastic creep to the mechanism of plastic creep with an increase in the magnetic field strength and the point defect concentration, as it is observed in our measurements. It has been shown that depinning current J_d rises with an increase in the point defect concentration. The elastic-creep activation energy quickly rises, while the plastic-creep activation energy decreases with a growing concentration of point defects. These peculiarities allow to explain evolution of the $J_c(H)$ dependence with irradiation dose in our measurements. At low fields the elastic-creep occurs, and increase in the n_{pd} enlarge both the depinning current and activation energy leading to increase of the measured current $J_c(H)$. At high fields the plastic-creep occurs, and increase in the n_{pd} enlarge the depinning current, but decreases activation energy [30]. Therefore the measured current $J_c(H)$ is determined by competition between increase in the J_d and decrease in the U. Below the peak position in the $J_c(H)$ curve increase in the J_d dominates over decrease in the U and therefore the measured current $J_c(H)$ increases with the irradiation dose. However below the peak position in the $J_c(H)$ curve decrease in the U dominates over increase in the J_d, and therefore the measured current $J_c(H)$ decreases with increased irradiation dose

3.3. THE ELECTRON IRRADIATION EFFECT ON CRITICAL CURRENT ANISOTROPY IN YBACUO SINGLE CRYSTALS

As it is known, owing to the laminated crystalline structure, the HTSC YBa_2Cu_3O single crystals show a substantial anisotropy of their properties, i.e., the difference between the parameters measured for different crystallographic directions of the crystal (e.g., electrical resistivity, critical current, etc.). The investigation of this phenomenon is of great importance for both the elucidation of mechanisms of high-T_c superconductivity and the practical use of HTSC materials in real devices and mechanisms One of the main challenges of this paper has been the investigation into the influence of electron irradiation on the critical current in HTSC single crystals, with the attention centered on the anisotropy of this parameter.

As indicated above in Section 2, to perform the studies, a special goniometric device was used. It provided the crystal orientation with respect to the electron beam during irradiation experiments, and relative to the external magnetic field during in situ measurements of current-voltage characteristics or electrical resistivity.

Fig. 5 shows the critical current of the single crystal as a function of crystal orientation relative to the 15 kOe external magnetic field vector. Curve 1 is for the initial sample, curves 2, and 3 are given for the sample irradiated to doses 10^{18} and $3\cdot10^{18}$ el/cm^2.

Let us consider the $J_{c1}(\alpha)$ curve for the nonirradiated crystal. Curve 1 shows three maxima (one for $\alpha = 0^\circ$, second for $\alpha \approx 50^\circ$, and third for $\alpha \approx 85^\circ$), and three minima (one for $\alpha \approx 14^\circ$, second for $\alpha \approx 71^\circ$, and third for $\alpha = 90^\circ$). The irradiation brings about cardinal changes in the critical current as a function of crystal orientation. A sharp rise in J_c is observed at the angle of 14°, for which the minimal critical current value of initial sample was measured. For the highest irradiation dose ($3\cdot10^{18}$ el/cm^2) the increase of critical current value is above 30 times. For crystal orientations between 50 and 85°, the introduction of point defects leads to an appreciable decrease in the critical current as compared to the nonirradiated sample. This effect increases with irradiation dose. For the angles close to 90°, i.e., for magnetic field vector oriented parallel to the **c** axis, a rise in the critical current is observed at the minimum dose 10^{18} el/cm^2, but further irradiation to $3\cdot10^{18}$ el/cm^2 causes a decrease in the critical current. Below we discuss possible reasons of these changes.

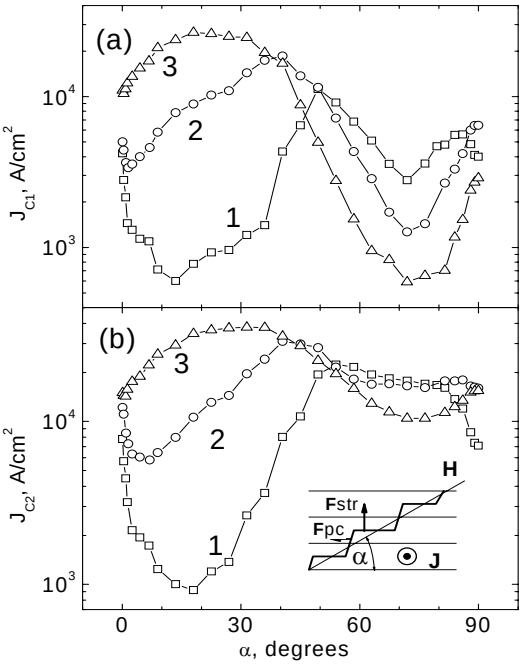

Fig. 5. Critical current J_{c1} (panel a) and J_{c2} (panel b) of the $YBa_2Cu_3O_{7-x}$ single crystal versus angle $\alpha \equiv \angle\mathbf{H}, ab$. Measurements were done at T = 85 K and H = 15 kOe before (curve 1) and after irradiation with doses 10^{18} (curve 2), and $3\cdot10^{18}$ (curve 3). The inset shows configuration of vortex line at small angles α

In anisotropic superconductors vortex structure depends on the anisotropy parameter ε and angle α. A rectilinear vortex structure obtains in magnetic fields $\mathbf{H}||ab$ and for angles $\alpha > \alpha_1 \approx \text{atan}(d/\xi)$. However, for angles $\alpha < \alpha_1 \approx \text{atan}(d/\xi)$ the rectilinear vortices transform into zigzag filaments, which finally form at angles $\alpha < \alpha_2 \approx \text{atan}\varepsilon$. The zigzag structure consists of vortex strings, oriented along the *ab* plane, which are

connected by "pancake" vortices, i.e. vortex fragments piercing the *ab* plane, as it is shown in the inset of Fig. 5.

Let us first discuss evolution of the $J_{c1}(\alpha)$ curve with irradiation dose at angles $\alpha < 15°$ where the zigzag structure is formed. The pinning of "pancake" vortices is determined by their interaction with structural defects. The nature of the pinning of "strings" depends on the orientation of the Lorentz force $\mathbf{F}_L=\mathbf{j}\times\mathbf{B}$. When the force $\mathbf{F}_L$ is oriented along the *ab* plane, the pinning is determined by the interaction with structural defects. However, when the Lorentz force is oriented along the **c** axis, the pinning force is finite even in the absence of any structural defects because of the presence of intrinsic pinning barriers due to the modulation of the superconducting order parameter along the **c** axis [31]. For our measurement geometry the Lorentz force acts on the strings along the *c* axis, and the "pancake" vortices, which carry the magnetic field component along this axis, can move along the *ab* plane independently of the strings. It is believed that pinning of "strings" is stronger compared to pinning of the "pancake" vortices due to strong intrinsic pinning barriers [20]. Therefore decrease of the current with increased angle α, which is realized in the nonirradiated sample, can be explained by decrease of pinning of the "pancake" vortices predicted by theoretical studies, $J_c \propto 1/\alpha$ [20].

Irradiation with a dose 10^{18} el/cm^2 cases nonmonotonous angular variation of the pinning force for angles $\alpha < 15°$. As can be seen in Fig. 5, the pinning force first decreases and then increases with increasing α. This nonmonotonic angle dependence of the pinning force is caused by transition from an ordered state of the VL at small angles α to a disordered state of the VL at larger angles α, i.e. minimum position $\alpha_{\min}$ on the $J_{c1}(\alpha)$ curve separates the ordered VL (formed at angles $\alpha < \alpha_{\min}$) and the ordered VL (formed at angles $\alpha > \alpha_{\min}$). Theoretical background of the OD transition induced by increase of angle α is given in Ref. [32]. The angular dependence of elastic energy required for the formation of displacements $u = c_L a_0$ has been calculated in terms of the cage potential model [13,14]. It has been shown that with the displacement orientation **u** along the *ab*-plane the energy $E_{el}^{\parallel} = c_L^2 \varepsilon \varepsilon_0 a_0$ is independent of the angle α. With the displacement orientation from the *ab*-plane, i.e., along the vector direction **B×(B×c)**, the energy $E_{el}^{\perp} = c_L^2 \varepsilon a_0 \varepsilon_0 / \varepsilon_\alpha$ decreases with an increasing angle α. At chaotic distribution of pinning centers, the displacements **u** comprise both parallel and perpendicular components. Therefore, the elastic energy will decrease with an increase in α due to the decreasing elastic energy required for the formation of the perpendicular component of transverse displacements. In the presence of point defects the pinning energy is independent of α. Therefore, at small angles α, the elastic energy may exceed the pinning energy value and the ordered state of the VL will be formed, whereas at large angles α the opposite relationship, $E_{el} < E_p$, may be fulfilled and then the disordered state of the VL will be formed. In this case, at a certain α_{OD} value the OD transition will be realized, and the angle α_{OD} value will be specified by the energy equality $E_{el}(\alpha_{OD}) = E_p(\alpha_{OD})$.

As it was mentioned above (section 3.2), in the OD transition the pinning force increases, this being due to the dimensional crossover (transition from 1D pinning of the ordered VL to 3D pinning of the disordered VL) and better adaptation of disordered VL to the landscape of pinning centers. So, it is reasonable to suggest that the position of minimum in the $J_{E1}(H)$ curve should correspond to the angle α_{OD}. This suggestion is supported by the decrease in the angle α_{OD} as the concentration n_{pd} increases. In fact, the n_{pd} increase leads to a rise in the pinning energy, $E_p \propto n_{pd}^{1/3}$, which may compensate a great loss of elastic energy, and thus, to the realization of OD transition at lower α values. Irradiation to a dose $3\cdot10^{18}$ el/cm^2 causes monotonous increase in the critical current with increasing angle (for angles $\alpha < 20°$), that indicates formation of disordered state of the VL at all angles α.

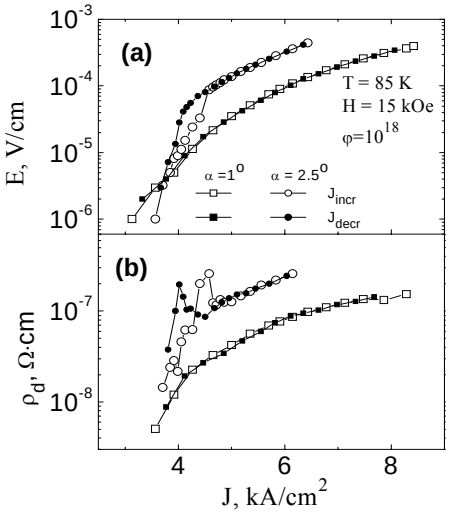

Fig. 6. Functions $E(J)$ and $\rho_d(J)$ measured at transport current increase and decrease (light and dark symbols, respectively)

Comparison of the $J_{c1}(\alpha)$ and $J_{c2}(\alpha)$ curves shows that their behavior at small angles α is qualitatively identical. However position of minimum on the $J_{c2}(\alpha)$ curve is shifted to higher angles compared to position of minimum on the $J_{c1}(\alpha)$ curve. This difference is analogous to the difference between the $J_{c1}(H)$ and $J_{c2}(H)$ curves, and can be explained by partial dynamic ordering of disordered VL. The theory predicts that the dynamic ordering of VL corresponds to the S-shaped $E(J)$ dependence and the presence of hysteresis in the $E(J)$ curves measured with increasing and decreasing current. It can be seen in Fig. 6 that with realization of the ordered VL state (at

$\alpha = 1° < \alpha_{OD} \approx 1.5°$) the electric field and dynamic resistance $\rho_d = dE(J)/dJ$ gradually increase with current, and the hysteresis is absent. In case of the disordered VL state realization (at $\alpha = 1° < \alpha_{OD}$) the $E(J)$ dependence take on the S shape, which is consistent with a nonmonotonic current dependence of the resistance ρ_d. Besides, the functions $E(J)$ measured with increasing and decreasing current show the hysteresis. Earlier, these regularities were experimentally observed at realization of the OD transition, which was caused by the magnetic field increase [27]. Within the framework of the "shaking temperature" model, the reason for $E(J)$ hysteresis is the "overheated" state of the ordered dynamic VL [21]. Therefore the OD transition occurring with a decreasing current is realized at a lower current value than in the case of the DO transition occurring with an increasing current.

Partial ordering of the dynamic VL reduces the pinning force that results in the displacement of the position of minimum in the angle dependence of pinning force towards higher angles α. This displacement is analogous to displacement of the minimum position to higher fields on the $J_{c2}(H)$ curve, compared to minimum position on the $J_{c1}(H)$ curve, that is observed in Fig.3.

We now discuss the results obtained at angles $\alpha > 15°$. Note that in the nonirradiated crystal with the field orientation $\mathbf{H} \| \mathbf{c}$ ($\alpha = 90°$) the single vortex pinning regime has been observed [30]. At this regime, the depinning current J_d and the creep activation energy U_0 are independent of the magnetic field value [20], i.e., the rate of vortex motion $\upsilon(J) = E(J)/cB$ is also independent of the field, and the elastic creep takes place. All these features indicate formation of the ordered state of VL. The introduction of point defects and the magnetic field rotation from the TBs plane involve transition to the plastic creep regime mediated by the VL dislocations motion, and the non-monotonous field variation of the pinning force. The transition from the single vortex pinning regime to the plastic mechanism of creep has been explained by OD transition [30]. As the defect concentration increases, the OD transition is realized owing to the increase in the pinning energy, $E_p \propto n_{pd}^{1/3}$ [20], that is likely to be higher in the irradiated sample than the elastic energy (1) necessary for the formation of transverse displacements $u = c_L a_0$. The OD transition in the non-irradiated sample, occurring as the field is rotated from the **c** axis (and hence, from the TB plane), arises due to the vortex line deformation in the vicinity of the TB. The amplitude of these displacements in absence of chaotic pinning centers equals [33]

$$u_{TB} \cong \left(\varepsilon a_0 / 2\sqrt{\pi}\right)\sqrt{\ln\left(a_0/\xi\right)}\sin(\theta_c - \theta) \approx \approx 0.1 a_0 \sin(\theta_c - \theta). \quad (2)$$

Here θ is angle between **H**-vector and TBs plane, the angles θ and α are related as $\sqrt{2}\sin\theta = \cos(\pi/2 - \alpha)$, and a critical angle θ_c defines region of angles $\theta < \theta_c$ where deformation of vortex lines near the TBs takes place. In the absence of the chaotic pinning potential the displacements (2) are less than $c_L a_0$ for the Lindemann number $c_L = 0.14$ [34]. In the presence of point defects (e.g., oxygen vacancies), the total amplitude of transverse deformations near the TB is given by the expression [33]

$$u_{TB,pd}(\theta) \approx \sqrt{u_{TB}^2(\theta) + u_{pd}^2(\theta)}, \quad (3)$$

where the u_{pd} component stems from the interaction with point defects. Apparently, in the nonirradiated crystal the u_{pd} component is less than the $c_L a_0$ value, but the amplitude (3) meets the Lindemann criterion, $u \geq c_L a_0$, and this just brings to the disordered VL formation in the fields inclined to the TB.

Considering these arguments, increase of the current J_c, observed in nonirradiated sample at the rotation of magnetic field off the TBs plane down to angle $\alpha \approx 85°$, can be explained by OD transition that improve adaptation of vortices to the pinning landscape. Further decrease of angle α down to 50° leads to non monotonous variation of the current J_{c1}, while the current J_{c2} continue increase, see Fig. 5. The same difference between the $J_{c1}(\alpha)$ and $J_{c2}(\alpha)$ dependences is observed in the angle range $40° < \alpha < 90°$ after irradiation with dose 10^{18} 1/cm^2, while after irradiation with dose $3 \cdot 10^{18}$ el/cm^2 both the $J_{c1}(\alpha)$ and $J_{c2}(\alpha)$ dependences are nonmonotonous in the angle range $30° < \alpha < 90°$. These peculiarities can be understood considering non-monotonous angular variation of the depinning current J_d and activation energy U_{pl} correspondent to the plastic creep, which are shown in Fig. 7. Methodology of determination of the depinning current and activation energy from measured $E(J)$ dependences is described in Refs. [33].

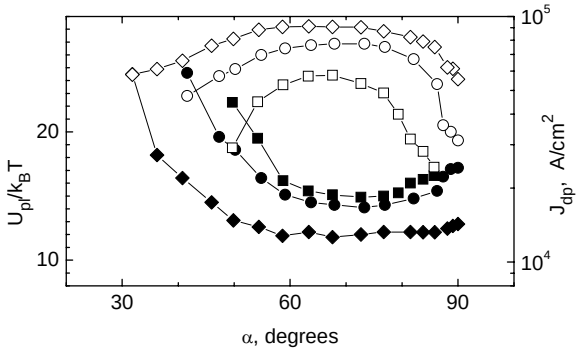

Fig. 7. Angular variation of the depinning current (light sybbols) and activation energy (dark symbols) before irradiation (squares), and after irradiation with doses 10^{18} (circles) and $3 \cdot 10^{18}$ (diamonds) [33]

Detailed analysis of non-monotonous $J_d(\alpha)$ and $U_{pl}(\alpha)$ dependences has been done in Ref. [33]. Hear we notice that $J_d(\alpha)$ dependence is primarily

controlled by non-monotonous variation of the correlation length L_0, i.e., longitudinal length of vortex line at which displacements $u = c_L a_0$ are independently formed. The $U_{pl}(\alpha)$ dependence is given by equation [33]

$$U_{pl}(\alpha) \approx U_{pl}^{\parallel} \cdot f(n_D) \cdot \left[1 - u_{TB,pd}(\theta)\right] \Big/ \sqrt{\varepsilon_\alpha}\ , \qquad (4)$$

where $U_{pl}^{\parallel} \approx 4\varepsilon\varepsilon_0 a_0$, $\varepsilon_\alpha = \sqrt{\sin^2\alpha + \varepsilon^2 \cos^2\alpha}$ is the anisotropy parameter dependent on α, and $f(n_D)$ is function dependent on concentration of the VL dislocations n_D. This function is controlled by the correlation length L_0, and it approaches unity in a strongly disordered VL and $f(n_D) \to \infty$ for the ordered VL.

As one can see, the depinning current and plastic-creep activation energy change in opposite way upon variation of both the angle α and the defects concentration. Increase of the defects concentration results in decrease of the activation energy, but in increase of the depinning current. Also, increasing and decreasing branches of the $U_{pl}(\alpha)$ dependence respectively correspond to decreasing and increasing branches of the $J_d(\alpha)$ dependence. Current-voltage characteristics inside the plastic creep regime are described by equation [29,33]

$$E(J) = \rho_0 J \exp\left[-\left(U_{pl}/kT\right)\left(1 - \sqrt{J/J_d}\right)\right] \qquad (5)$$

and therefore variation of measured currents J_{c1} and J_{c2}, which characterize pinning at voltage criteria $E = const$, is determined by competition between variation of the activation energy and the depinning current.

Comparison of data presented in Fig. 5 and Fig. 7 shows that variation of measured current J_{c1}, which characterizes pinning force deep inside creep regime, is primarily controlled by variation of the plastic-creep activation energy. However variation of the current J_{c2}, which characterizes pinning force at higher value of the voltage criteria, depends on particular variation of both the depinning current and activation energy.

3.4. EVOLUTION OF CRITICAL CURRENT ANISOTROPY WITH TEMPERATURE

To clarify the special features in the influence of the temperature on critical current anisotropy, we have measured the $J_{c2}(\alpha)$ dependence in the magnetic field $H = 15$ kOe for $T = 81$ K. The measurements were performed before and after irradiation to a dose of $3 \cdot 10^{18}$ el/cm^2. Result of measurements is presented in Fig. 4. This figure also shows the $J_{c2}(\alpha)$ dependence measured in the magnetic field $H = 15$ kOe for $T = 85$ K.

Comparison of the currents $J_{c2}(81\ K)$ and $J_{c2}(85\ K)$ lead us to the following conclusions. Decrease in the temperature from 85 K down to 81 K leads to a substantial increase (by factors of 1.6 to 3.4) in the pinning force. At $T = 81$ K the irradiation does not practically affect the critical current value for $\alpha = 0^\circ$, but has considerably increased J_c for all other crystal orientations, even for the 50…85° range, for which a decrease in the critical current at 85 K is observed. The maximum relative increase in the critical current due to irradiation is observed for the orientation $\alpha = 14°$. For $T = 85$ K this increase in the critical current equals 32.4, and for $T = 81$ K the increase equals 15.5, i.e. two times smaller. The influence of low-temperature electron irradiation on the anisotropic behavior of critical current in the $YBa_2Cu_3O_{7-x}$ single crystal suggests the following interpretation.

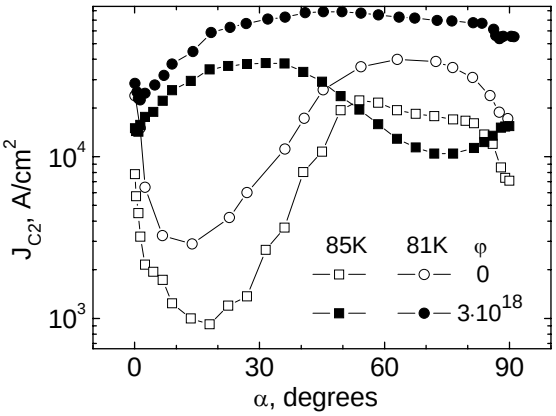

Fig. 8. Angular variation of the critical current measured at T = 85 K and T = 81 K in magnetic field H = 15 kOe before irradiation and after irradiation with a dose of $3 \cdot 10^{18}$ el/cm^2

As can be seen in Fig. 8, at temperature 81 K the $J_{c2}(\alpha)$ dependence has local minimum at $\alpha = 1.4°$. This is evidence that the ordered state of the VL occurs for angles of $\alpha < 1.4°$, whereas the disordered state of the VL occurs in the same region of angles at T=85 K. This difference is caused by the fact that the elastic energy increases with decreasing temperature more rapidly than the pinning energy [13]. Therefore, when the temperature decreases (while the field and angle α are kept constant), a transition occurs from the disordered to the ordered state.

In magnetic field applied parallel to the *ab*-plane ($\alpha = 0^\circ$) pinning force is strong due to presence of intrinsic pinning buriers, and introduction of additional point-like pinning centers slightly increases (about 1.2 and 2 times respectively for 81 and 85 K) the critical current. For angles $\alpha > 40°$ pinning force is strongly affected by twins, and introduction of additional point defects slightly increases the critical current at 81 K, and slightly decreases the critical current at 85 K. Decisive role of the point defects is seen in the range of angles $1° < \alpha < 40°$, where intrinsic pinning and pinning at twin boundaries "do not work". This conclusion is verified by the results of our studies into the influence of low-temperature irradiation on the transformation of anisotropic dependences of the critical current. Really, the 2.5 MeV electron irradiation generates only point defects in the single crystal lattice, and possibly, taking into account the annealing of irradiated samples at 100 K, small point-defect clusters. With an increasing irradiation dose, i.e., with an

increase in the point defect concentration, the maximum increments in the critical current are observed just for the above-mentioned crystal orientation. A decrease of critical current in the irradiated specimens at 85 K for the range $1° < \alpha < 40°$ may be due to an appreciable decrease in the melting temperature of the superconductor vortex lattice, (T_m). At $T = T_m$ the ohmic superconducting-normal transition begins with a dramatic falloff of critical current to zero. As shown in Section 3, for the 50…85° orientation, T_m differs from the temperature of measurements by no more than 2 K. Therefore, even a 1 to 1.5 K decrease in the melting temperature due to irradiation leads to an essential drop in the critical current. The conclusion is verified by the measurements for 81 K (Section 5, Fig. 3). In this case, the measurement temperature is 5 to 6 K below the T_m for $\alpha = 50…85^{\circ}$, and irradiation provides a rise in the critical current for all crystal orientations, including the range under consideration. Note, that effect of melting manifests itself in decrease of the activation energy, while the depinning current increases with the irradiation dose, see Fig. 7.

3.5. THE DEPENDENCE OF CRITICAL CURRENT ON THE RADIATION DOSE

The low-temperature irradiation with 2.5 MeV electrons provides precision studies into the influence of point defect concentration on the critical current of HTSC single crystals. Below, we consider and analyze dose dependence of the critical current shown in Fig. 9. As it follows from the data, the relative increase in the critical current $J_c(\varphi)/J_c(0)$ with the irradiation dose depends on the temperature, magnetic field and angle α.

For the maximum dose ($3.1\cdot10^{18}$ el/cm^2) and $\alpha = 14°$ the ratio $J(\varphi)/J(0)$ attains the following values: 8.7 (for 77 K), 11.5 (79 K), 22.1 (83 K) and 31.4 (86 K). In this case, the absolute J_{cirr} values make 63.6, 54.05, 37.4 and 25.2 kA/cm^2, respectively. Except for the "zero dose", all the dependences can be fairly approximated by the straight lines. This is conformed with the slope $k = 1$ observed for dose dependence of the relative critical current $J(\varphi)/J(0)$ being re-plotted in the $\ln[J_c(\varphi)/J_c(0)] - \ln\varphi$ scale, see Fig. 10. The linear approximation to high radiation doses allows us to predict a certain critical current value of the irradiated single crystals. Thus it can be expected that $J_c = 100$ kA/cm^2 at 77 K can be attained after irradiation to a dose of $(5.5…6.0)\cdot10^{18}$ el/cm^2. This critical current value is a record for HTSC YBaCuO single crystals for their possible operation at a liquid nitrogen temperature (77 K) in the field $H = 10$ kOe. The relative increase in the critical current, as compared to the initial (nonirradiated) sample, is expected to be 8.7 The same-level critical current (100 kA/cm^2) for 86 K can be attained at irradiation to a dose of $1\cdot10^{19}$ el/cm^2. This will make a nearly 100-fold relative increase. However, the dose curve for this temperature may deviate from the linear dependence due to the fact that with an increase in the radiation defect concentration the melting temperature of the vortex lattice will approach the temperature of critical current measurement. For lower temperatures of measurement this effect will exert a substantially less influence.

For the maximum irradiation dose ($3.1\cdot10^{18}$ el/cm^2), magnetic field 15 kOe, and $\alpha = 0$ the ratio $J_c(\varphi)/J_c(0)$ attains the values 2.7 (for 85 K) and 1.2 (for 81 K), i.e., they are much smaller compared to the ratio values $J_c(\varphi)/J_c(0)$ obtained for $\alpha = 14°$. This difference is plausible considering presence of strong intrinsic pinning barriers, which give substantial contribution to the pinning force in magnetic field applied parallel to *ab*-plane of the crystal. Therefore increase of the point defects concentration slight increases the pinning force.

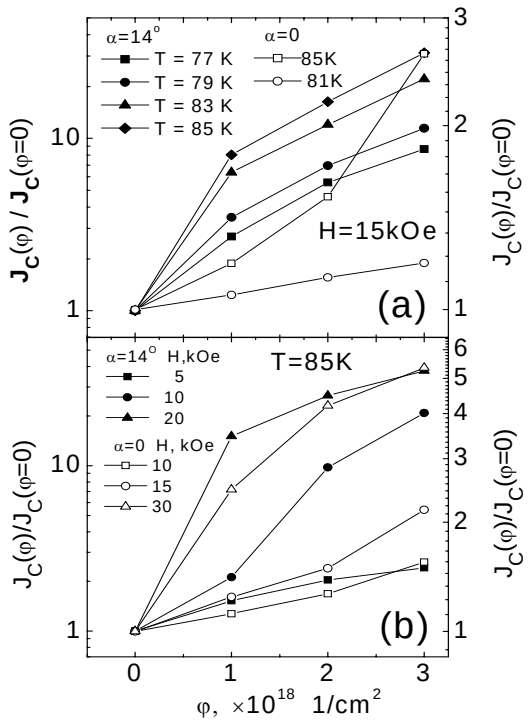

Fig. 9. Dose dependences of relative increase of the critical current

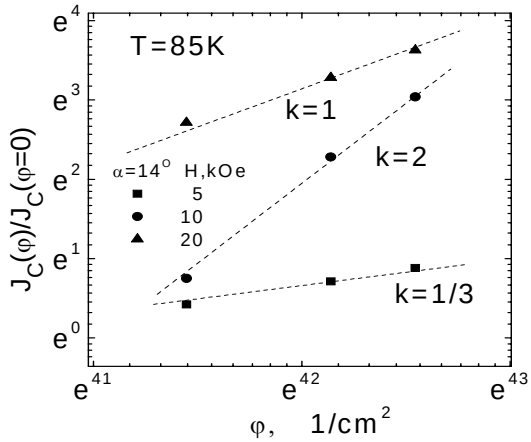

Fig. 10. Dose dependences of relative increase of the critical current plotted in double logarithmic scale

It is important to notice difference in dose dependence of the ratio $J(\varphi)/J(0)$, which is observed in different magnetic fields for angle $\alpha = 14°$. In magnetic field 5 kOe the ratio weak increases with dose,

and the slope $k = 1/3$, see Fig. 10, corresponds to dose dependence of the pinning force $F_p \propto n_{pd}^{1/3}$ in agreement with predictions of the collective pinning theory for the single vortex pinning regime [20]. As seen in Fig. 3, pinning force decreases with increasing field up to 5 kOe, i.e., ordered VL is formed for all irradiation dose. Therefore weak increase of the pinning force with the defects concentration, $F_p \propto n_{pd}^{1/3}$, is characteristic feature of the ordered VL.

In magnetic field 20 kOe the ratio $J(\varphi)/J(0)$ sharp increases at irradiation to a dose of 10^{18} el/cm^2, and steady increases with further dose increase, that is conformed in the slope $k = 1$, see Fig. 10, i.e., in dose dependence of the pinning force $F_p \propto n_{pd}$. The field 20 kOe is far above H_{OD} for all irradiation dose. Therefore sharp increase of the ratio occurred after irradiation to a dose of 10^{18} el/cm^2 can be attributed to transition from the ordered to disordered state of VL, and steady increase of the pinning force $F_p \propto n_{pd}$ can be attributed to characteristic feature of the ordered VL formed far above the OD transition.

In magnetic field 10 kOe the ratio $J(\varphi)/J(0)$ weak increases at irradiation to a dose of 10^{18} el/cm^2, and fast increases with further increase in the dose, that is conformed in the slope $k = 2$, see Fig. 10, i.e., in dose dependence of the pinning force $F_p \propto n_{pd}^2$. As seen in Fig. 3, pinning force decreases with increasing field up to 10 kOe, i.e., for this irradiation dose ordered VL is formed. Further increase in the irradiation dose leads to decrease of minimum position on the $J_c(H)$ curves below 10 kOe, see Fig. 3, indicating formation of disordered VL, therefore fast increase in the pinning force with the $F_p \propto n_{pd}^2$ is characteristic feature of the disordered VL formed just above the OD transition.

Thus we can conclude that increase of point defects concentration cause weak increase of the pinning force of the ordered VL, sharp (parabolic) increase of the pinning force at the OD transition, and steady (linear) increase of the pinning force of the disordered VL far above the OD transition. Analogous qualitative variation of the pinning force (the same exponents of power) is observed for magnetic field applied parallel to the *ab*-plane of the crystal, though relative increase of the pinning force is much smaller.

3.6. THE DEPENDENCE OF CRITICAL CURRENT ON THE ANNEAL OF IRRADIATION DEFECTS

Previous experimental studies have shown that structure defects produced by the low-temperature (10 K) irradiation with 2.5 MeV electrons are partially annealed upon increase of temperature [35]. However, sme part of the irradiation defects is stable at such high temperature as 350 K. Our results, which are shown in Fig. 11, support this conclusion. It is seen, that anneal of the irradiated sample at 330 K partially decreases the critical current, but it remains higher compared to critical current in the initial (non-irradiated) crystal.

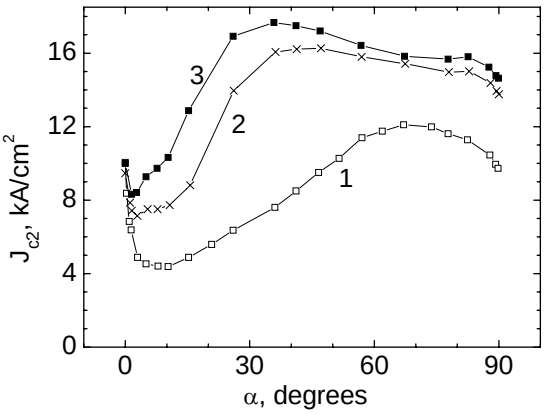

Fig. 11. Angular variation of the critical current measured at T = 81 K in magnetic field H = 15 kOe before irradiation (curve 1), after irradiation with a dose of 2.3·10^{18} el/cm^2 and after subsequent anneal of the sample at T=330 K

4. CONCLUSIONS

- Investigations have been performed to elucidate the influence of low-temperature electron irradiation on the superconductor critical temperature and the transport critical current in high-quality HTSC single crystals.
- The evolution of critical temperature and melting temperature has been investigated versus irradiation dose and the crystal orientation relative to the magnetic field.
- Detailed studies have been made into evolution of the critical current with radiation defects concentration: the current slow increases for ordered vortex lattice ($J_c \propto n_{pd}^{1/3}$), fast increases just above the transition into the disordered state of vortex lattice ($J_c \propto n_{pd}^2$), and steady increase is observed for disordered vortex lattice.
- Detailed investigations have been made into evolution of the critical current with magnetic field and angle α between magnetic field vector and crystallographic *ab*-plane of the crystal. Both the $J_c(H)$ and $J_c(\alpha)$ functions are dependent on the phase state of vortex lattice. Role of radiation-induced point defects and planar defects (twin boundaries) in formation of the phase state of the vortex lattice has been elucidated.
- It has been demonstrated that the point defects, generated by electron irradiation, are the efficient pinning centers in HTSC single crystals, and they are responsible for a substantial rise in the critical current. The maximum (more than 30-fold) relative increase in the critical current has been obtained for the YBaCuO single crystal irradiated to a dose of 3·10^{18} el/cm^2, the crystallographic *ab*-plane being oriented at $\alpha = 14°$ with respect to the external magnetic-field vector.
- For the conditions of maximum effect of irradiation, dose dependences of critical current have been investigated for different temperatures of measurement. Relying on the approximation of the experimental dependences obtained, a conclusion was

made about the possibility of increasing the critical current density up to 10^5 A/cm^2 at 77 K in single crystals irradiated with 2.5 MeV electrons to a dose of ~ (5.5…6)·10^{18} el/cm^2.

• The present data on the efficient influence of electron irradiation on the critical current increase in HTSC single crystals can be used in the development of the principles of radiation technology of increasing the intragranular critical current in bulk polycrystalline high-T_c superconductors for their use in new devices and mechanisms.

ACKNOWLEDGEMENT

Author is grateful Valeriy Borysenko for carry out electron irradiation and experimental measurements, and to Aleksandr Bondarenko for helpful discussions and critical reading of the manuscript.

REFERENCES

1. D. Bruce Montgomery. The future prospects for large-scale applications of superconductivity // *Superconductivity: Research and Development*. 1998, N 9-10, p 78-92.
2. L.K. Kovalev et al. HTS motors design. Recent results and future development // *Superconductivity: Research and Development*. 1998, N 9-10, p.69-77.
3. F.M. Sauerzopf, H.P. Wiesinger, H.W. Weber, G.W. Crabtree, M.C. Frischherz, and M.A. Kirk. Anisotropic shift of the irreversibility line by neutron irradiation // *Supercond. Sci. Technol.* 1992, v. 5, S105-108.
4. W. Kritscha, F.M. Sauerzopf, H.W. Weber, G.W. Crabtree, Y.C. Chang, and P.Z. Jiang. Critical Currents and Magnetization of $Bi_2Sr_2CaCu_2O_8$ Single Crystals // *Supercond. Sci. Technol.* 1992, v.5, p.232-235.
5. A. Wisniewski, R. Puzniak, J. Karpinski, J. Hofer, R. Szymczak, M. Baran, F.M. Sauerzopf, R. Molinski, E.M. Kopnin, J.R. Thompson. Influence of neutron-irradiation-induced defects on the flux pinning inHgBa2Ca2Cu3O8+x single crystals // *Phys.Rev.B.* 2000, v.61, p.791.
6. L. Civale, A.D. Marwick, T.K. Worthington, M.A. Kirk, J.R Thompson, L. Krusin-Elbaum, Y. Sun, J.R. Clem, and F. Holtzberg. Vortex confinement by columnar defects in $YBa_2Cu_3O_7$ crystals: Enhanced pinning at high fields and temperatures // *Phys.Rev.Lett.* 1991, v.67, p.648.
7. D.R. Nelson and V.M. Vinokur. Boson localization and correlated pinning of superconducting vortex arrays // *Phys.Rev.B.* 1993, v.48, p.13060.
8. J.R. Thompson et al. Current-density enhancements of the highest-Tc superconductors with GeV protons *// Appl.Phys.Lett.* 1997, v.71, p.536.
9. L.M. Paulius, J.A. Fendrich, W.-K. Kwok, A.E. Koshelev, V.M. Vinokur, G.W. Crabtree B.G. Glagola. Effects of 1-GeV uranium ion irradiation on vortex pinning in single crystals of the high-temperature superconductor $YBa_2Cu_3O_{7-\delta}$ // *Phys.Rev.B.* 1997, v.56, p.913.
10. M.A. Obolenskii, A.V. Bondarenko, V.I. Beletskij, et al. Syntesys and physical properties of $YBa_2Cu_3O_{7-\delta}$ syngle crystals // *Sov. J. Low Temp. Phys.* 1990, v.16, p.639.
11. F. Dworschak, U. Dedek, and Yu. Petrusenko. Anisotropy of defect production in YBaCuO single crystals irradiated with 3 MeV electrons // *Physica C.* 1994, v.235-240, p.1343.
12. J. Giapintzakis, W.C. Lee, J.P. Rice, D.M. Ginsberg, I.M. Robertson, R. Wheeler, M. A. Kirk, M.O. Ruault. Production and identification of flux-pinning defects by electron irradiation in $YBa_2Cu_3O_{7-x}$ single crystals // *Physical Review B.* 1992, v.45, p.10677.
13. D. Ertas and D.R. Nelson. Irreversibility, mechanical entanglement and thermal melting in superconducting vortex crystals with point impurities // *Physica C.* 1996, v.272, p.79.
14. V. Vinokur, B. Khaikovich, E. Zeldov, M. Konczykowski, R.A. Doyle, P.H. Kes. Lindemann criterion and vortex-matter phase transitions in high-temperature superconductors // *Physica C*. 1999, v.295, p. 209.
15. R. Cubbit, E.M. Forgan, G. Yang, S.L. Lee, D. Paul, H.A. Mook, M. Yethiraj, P.H. Kes, T.W. Li, A.A. Menovsky, Z. Tarnavski, and K. Mortensen // *Nature.* 1993, v.365, p.407.
16. Terukazu Nishizaki, Kenji Shibata, Makoto Maki, Norio Kobayashi. STM/STS studies on vortex and electronic state in $YBa_2Cu_3O_y$ // *Physica C*. 2006, v. 437-438, p. 220-225.
17. B. Khaikovich, E. Zeldov, D. Majer, T.W. Li, P.H. Kes, and M. Konczykovski. Vortex-Lattice Phase Transitions in $Bi_2Sr_2CaCu_2O_8$ Crystals with Different Oxygen Stoichiometry // *Phys. Rev. Lett*. 1996, v.76, p.2555.
18. R. Wordenweber and P.H. Kes. Dimensional crossover in collective flux pinning // *Phys. Rev. B*. 1986, v.34, p.494.
19. T. Giamarchi and P.Le Doussal. Phase diagrams of flux lattices with disorder //*Phys. Rev. B.* 1997, v.55, p.6577.
20. G. Blatter, M.V. Feigel'man, V.B. Geshkenbein, A.I. Larkin, and V.M. Vinokur. Vortices in high-temperature superconductors // *Rev. Mod. Phys.* 1994, v.66, p.1125.
21. A.E. Koshelev and V.M. Vinokur. Dynamic melting of the vortex lattice // *Phys. Rev. Lett.* 1994, v.73, N 26, p. 3580 - 3583.
22. T. Giamarchi and P.Le Doussal. Moving glass phase of driven lattices // *Phys. Rev. Lett*. 1996, v.76, N 18, p. 3408 - 3411.
23. M. Marchevsky, J. Aarts, P.H. Kes, M.V. Indenbom. Observation of the correlated vortex flow in $NbSe_2$ with magnetic decoration // *Phys.Rev.Lett.* 1997, v.78, N 3, p. 531–534.
24. K. Moon, R.T. Scalettar, and G.T. Zimanyi. Dynamical phases of driven vortex system // *Phys.Rev.Lett.* 1996, v.77, N 13, p. 2778-2781.
25. N. Kokubo, T. Asada, K. Kadowaki, K. Takita, T.G. Sorop, and P.H. Kes. Dynamic ordering of driven vortex matter in the peak effect regime of amorphous MoGe films and 2H-$NbSe_2$ crystals // *Phys. Rev. B*. 2007, v.75, p.184512.

26. A.A. Gapud, D.K. Christen, J.R. Thompson, and M.Yethiraj. Electrical transport, magnetic, and structural properties of the vortex lattice of V_3Si in the vicinity of the peak effect // *Phys. Rev. B,* 2003, v.67, p.104516.
27. A.V. Bondarenko, A.A. Zavgorodnij, D.A. Lotnik, M.A. Obolenskii, R.V. Vovk, and Y. Biletskiy. Creep and depinning of vortices in non twinned $YBa_2Cu_3O_{6.87}$ single crystal // *Fiz. Nizk. Temp.* 2008, v.34, p.645.
28. Yu.T. Petrusenko. Static and dynamic order-disorder transition of vortexlattice in YBaCuO crystals: The effect of point defects, anisotropy, temperature, and magnetic field // *Low Temperature Physics*. 1998, v.36, №1, p.105.
29. Y. Abulafia, A. Shaulov, Y. Wolfus, R. Prozorov, L. Burlachkov, Y. Yeshurun, D. Majer, E. Zeldov, H. Wühl, V.B. Geshkenbein, V.M. Vinokur. Plastic Vortex Creep in $YBa_2Cu_3O_{7-x}$ Crystals // *Phys. Rev. Lett.* 1996, v.**77**, p.1596.
30. A.V. Bondarenko, A.A. Prodan, Yu.T. Petrusenko, V.N. Borisenko, F. Dworschak, and U. Dedek. Effect of electron irradiation on vortex dynamics in $YBa_2Cu_3O_{7-\delta}$ single crystals // *Phys. Rev. B.* 2001, v.64, p.092513.
31. M. Tachiki and S. Takahashi // *Solid State Commun*. 1989, v.70, p.291.
32. Yu.T. Petrusenko, A.V. Bondarenko. Pinning and dynamics of vortices in $YBa_2Cu_3O_{7-\delta}$ crystal in magnetic field applied in vicinity of the ab plane: the effect of point defects // *Fiz. Nizk. Temp*. 2009, v.35, N 2, p. 159-163.
33. Yu.T. Petrusenko, A.V. Bondarenko. Interplay of point and planar defects in the phase state formation and dynamics of Abrikosov vortices in $YBa_2Cu_3O_{7-\delta}$ crystals // *Functional Materials*. 2009, v.16, N 1, p.11.
34. W.K. Kwok, J.A. Fendrich, S. Flesher, U. Welp, J. Downey, G.W. Crabtree. Vortex liquid Disorder and the First Order Melting Transition in $YBa_2Cu_3O_{7-\delta}$ // *Phys. Rev. Lett*. 1994, v.72, N 7, p.1092.
35. Yu.T. Petrusenko, A.V. Bondarenko, A.M. Kozyrenko, S.M. Shkirida. Anisortopic character of the defects and recovery processes in twinned $YBa_2Cu_3O_{7-\delta}$ crystals irradiated with 0.5…2.5 MeV electrons // *Problems of Atomic Science and Technology. Series: «Physics of Radiation Effect and Radiation Materials Science».* 2010, №1, p. 42-48.

Статья поступила в редакцию 12.07.2010 г.

УГЛОВЫЕ И МАГНИТНО-ПОЛЕВЫЕ ЗАВИСИМОСТИ КРИТИЧЕСКОГО ТОКА ОБЛУЧЕННЫХ МОНОКРИСТАЛЛОВ YBaCuO

Ю. Петрусенко

Проведено исследование механизмов, ответственных за токонесущую способность облученных высокотемпературных сверхпроводников (ВТСП). Для этого были выполнены эксперименты по изучению влияния генерированных облучением высокоэнергетичными электронами точечных дефектов на температуру сверхпроводящего перехода и критический ток ВТСП-монокристаллов $YBa_2Cu_3O_{7-x}$. Критический транспортный ток в монокристаллах определялся с помощью метода пропускания постоянного тока плотностью до 80000 А/см^2. Экспериментально установлено более чем 30-кратное увеличение плотности критического тока в монокристаллах, облученных электронами с энергией 2,5 МэВ до дозы $3\cdot10^{18}$ эл./см^2. Проведены детальные исследования анизотропии критического тока и его зависимости от величины магнитного поля в облученных монокристаллах. Впервые показана высокая эффективность точечных дефектов как центров пиннинга магнитных вихрей в ВТСП-монокристаллах.

КУТОВІ ТА МАГНІТНО-ПОЛЬОВІ ЗАЛЕЖНОСТІ КРИТИЧНОГО СТРУМУ ОПРОМІНЕНИХ МОНОКРИСТАЛІВ YBaCuO

Ю. Петрусенко

Проведено дослідження механізмів, що обумовлюють струмонесучу спроможність опромінених високотемпературних надпровідників (ВТНП). В роботі виконані експерименти з встановлення впливу генерованих опроміненням високоенергетичними електронами точкових дефектів на температуру надпровідного переходу та критичний струм у ВТНП-монокристалах $YBa_2Cu_3O_{7-x}$. Критичний транспортний струм в монокристалах вимірювався з використанням методу перепускання постійного струму щільністю до 80000 А/см^2. Експериментально встановлено більш ніж 30-разове підвищення щільності критичного струму в монокристалах, що опромінені електронами з енергією 2,5 МеВ дозою $3\cdot10^{18}$ ел./см^2. Виконані детальні дослідження анізотропії критичного струму і його залежності від величини магнітного поля в опромінених монокристалах. Вперше показана висока ефективність точкових дефектів як центрів пінінгу магнітних вихорів у ВТНП-монокристалах.